The Astrophysical Journal Letters, 744:L2 (5pp), 2012 January 1 doi:10.1088/2041-8205/744/1/L2

FERMI LARGE AREA TELESCOPE DETECTION OF THE YOUNG SUPERNOVA REMNANT TYCHO

F. Giordano[1,2], M. Naumann-Godo[3], J. Ballet[3], K. Bechtol[4], S. Funk[4], J. Lande[4], M. N. Mazziotta[2], S. Rainò[2], T. Tanaka[4], O. Tibolla[5], and Y. Uchiyama[4]

[1] Dipartimento di Fisica, "M. Merlin" dell'Università e del Politecnico di Bari, I-70126 Bari, Italy
[2] Istituto Nazionale di Fisica Nucleare, Sezione di Bari, 70126 Bari, Italy; francesco.giordano@ba.infn.it
[3] Laboratoire AIM, CEA-IRFU/CNRS/Université Paris Diderot, Service d'Astrophysique, CEA Saclay, 91191 Gif sur Yvette, France; Melitta.Naumann-Godo@cea.fr
[4] W. W. Hansen Experimental Physics Laboratory, Kavli Institute for Particle Astrophysics and Cosmology, Department of Physics and SLAC National Accelerator Laboratory, Stanford University, Stanford, CA 94305, USA
[5] Institut für Theoretische Physik and Astrophysik, Universität Würzburg, D-97074 Würzburg, Germany
Received 2011 July 29; accepted 2011 October 26; published 2011 December 7

ABSTRACT

After almost three years of data taking in sky-survey mode, the *Fermi* Large Area Telescope has detected γ-ray emission toward Tycho's supernova remnant (SNR). The Tycho SNR is among the youngest remnants in the Galaxy, originating from a Type Ia Supernova in AD 1572. The γ-ray integral flux from 400 MeV up to 100 GeV has been measured to be $(3.5 \pm 1.1_{\rm stat} \pm 0.7_{\rm syst}) \times 10^{-9}$ cm^{-2} s^{-1} with a photon index of $2.3 \pm 0.2_{\rm stat} \pm 0.1_{\rm syst}$. A simple model consistent with TeV, X-ray, and radio data is sufficient to explain the observed emission as originating from π^0 decays as a result of cosmic-ray acceleration and interaction with the ambient medium.

Key words: acceleration of particles – radiation mechanisms: non-thermal – supernovae: individual (Tycho)

Online-only material: color figures

1. INTRODUCTION

Tycho's supernova remnant (SNR: SN 1572 or SNR120.1+01.4) is classified as a Type Ia (thermonuclear explosion of a white dwarf) based on observations of the light-echo spectrum (Krause et al. 2008; Rest et al. 2008). Its expansion has been observed in the radio (Very Large Array; Reynoso et al. 1999) and X-rays (*Chandra*; Katsuda et al. 2010). The average expansion parameter is $\nu = 0.47$ (radio) to 0.52 (X-rays) and shows strong azimuthal variations. Along three-quarters of the rim it is consistent with $\nu = 4/7$, expected from a reverse shock developing into r^{-7} ejecta (Chevalier 1982), while toward the east it is much lower, probably due to recent deceleration in a higher density medium. The shock speed is approximately 1400 $D_{\rm kpc}$ km s^{-1}, except toward the east.

Tycho's distance is not very well constrained. H I absorption studies (Tian & Leahy 2011) favor a distance on the near side of the Perseus arm (2.5 to 3 kpc). On the other hand, Hayato et al. (2010) measured the shocked ejecta velocity to be about 4700 km s^{-1} for Si, S, and Ar. They concluded that the distance is 3 to 5 kpc on consideration of the measured proper motion.

The radio flux (Kothes et al. 2006) is 40.4 Jy at 1.4 GHz with a spectral index of 0.65. The overall X-ray spectrum (Decourchelle et al. 2001) is dominated by very strong line features of Si, S, and Fe arising in the shocked ejecta. However, majority (60%) of the X-ray continuum emission comes from non-thermal synchrotron rather than thermal bremsstrahlung (Warren et al. 2005), and non-imaging instruments indicate that it extends to more than 10 keV (Fink et al. 1994; Petre et al. 1999). Recently, the VERITAS ground-based telescope reported a TeV detection with a flux of 0.9% of the steady Crab Nebula (Acciari et al. 2011).

Several arguments point toward a cosmic-ray-modified shock in Tycho. Warren et al. (2005) have argued that the contact discontinuity between the ejecta and the shocked ambient medium is too close to the blast wave for a compression factor of four. The other important hint comes from the narrow width of the X-ray synchrotron rims, which is probably due to fast cooling of the accelerated electrons behind the blast wave, and requires the magnetic field to be amplified by accelerated particles to 200 μG (Cassam-Chenaï et al. 2007). Recent optical observations of a fast shock in Tycho have even provided the first observational indications of a cosmic-ray precursor (Lee et al. 2010).

In this Letter, we report the GeV detection of Tycho's SNR with the *Fermi* Large Area Telescope (LAT).

2. OBSERVATIONS AND DATA REDUCTION

The *Fermi Gamma-ray Space Telescope*, launched in 2008 June, has operated almost exclusively in sky-survey mode since 2008 August 4. The principal *Fermi* scientific instrument, the LAT has a wide field of view of 2.4 sr, which allows it to observe the whole sky every ~3 hr (two orbits), a large effective area of ~8000 cm^2 (on-axis at 1 GeV) and a point-spread function (PSF) narrower than 1.°0 (for 68% containment) at 1 GeV. For a detailed description of the instrument see Atwood et al. (2009).

We have selected a data set of 34 months in a square region of interest (RoI) of 20° side length, centered on the position of the remnant, selecting events from 400 MeV to 100 GeV in the *P6_DIFFUSE* class.[6] The choice of selecting events above 400 MeV is motivated by the broad PSF at low energy (≈5° at 100 MeV). Moreover, the SNR is only 1.°4 from the Galactic plane, a region mainly dominated by low-energy photons from the Galactic diffuse emission, which makes the low-energy analysis particularly difficult and subject to large systematics uncertainties.

In addition, to limit contamination from photons produced by cosmic-ray interactions in the upper atmosphere, a 105° cut on the Earth zenith angle has been applied (Abdo et al. 2009).

3. ANALYSIS AND RESULTS

The γ-ray spectrum from a point-like source coincident with the Tycho SNR has been obtained using the Fermi Science

[6] http://www.slac.stanford.edu/exp/glast/wb/prod/scienceAnalysis_Home.htm

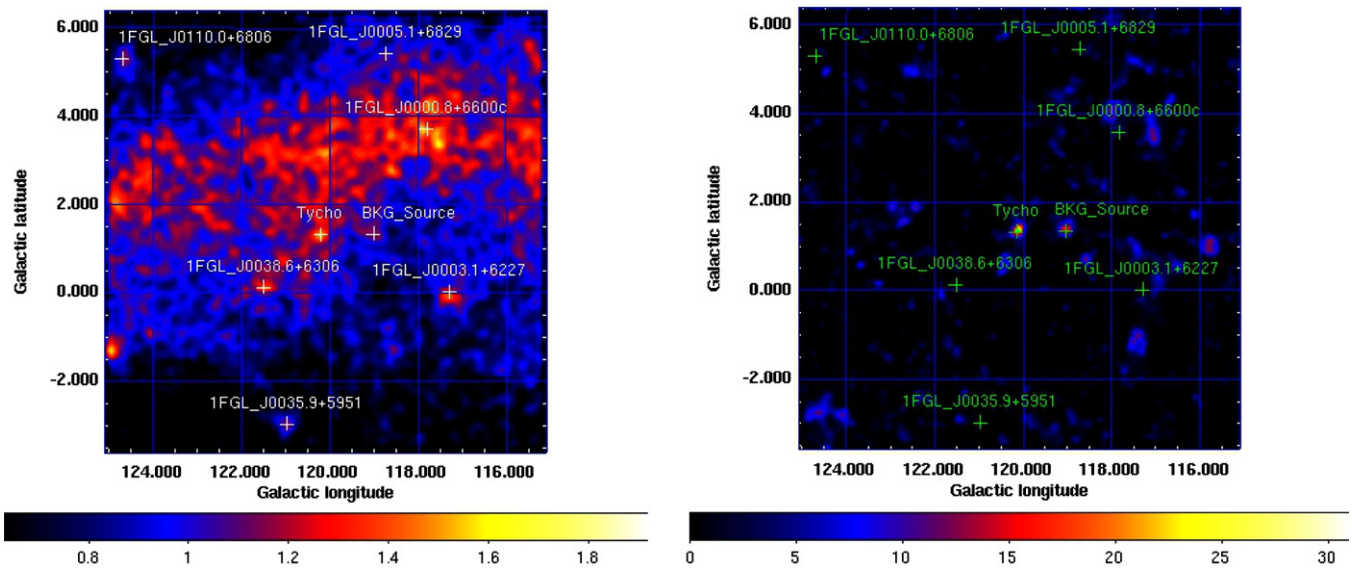

Figure 1. Left: *Fermi*-LAT count map of the $10^\circ \times 10^\circ$ region for photons above 1 GeV. The crosses indicate the point-like sources included in the model for the fit. A Gaussian smoothing of $0\overset{\circ}{.}3$ has been applied. Right: map of the likelihood TS (i.e., map of the TS values obtained for a test source that has been stepped through a grid of positions, with the likelihood re-optimized at each position) of the same region for photons above 1 GeV. All contributions from known sources and diffuse emission have been included in the source model and so are not apparent here except Tycho, which corresponds to the bright spot (TS = 33) in the center of the image.
(A color version of this figure is available in the online journal.)

Tool *gtlike* publicly available from the Fermi Science Support Center.[7] The *gtlike* tool has been used in binned mode. The analysis method consists of fitting all sources in the RoI assuming a simple power-law model in the selected energy interval; both the integral flux and the photon index of each source within 5° of Tycho's SNR are kept free in the fit. Only the pulsar PSRJ0007+7303 in the CTA1 SNR has been fitted with a power law with an exponential cutoff. Moreover, all point-like sources included in the 1FGL catalog (Abdo et al. 2010a) and located within the selected RoI have been accounted for (Figure 1 left). The diffuse emission, including the emission from our Galaxy and an isotropic component, is modeled according to the gll_iem_v02_P6_V11_DIFFUSE.fit[8] optimized for the Instrument Response Functions (IRFs) *P6V11*. The right panel of Figure 1 shows the map of the likelihood Test Statistic (TS)[9] for $E > 1$ GeV of a $10^\circ \times 10^\circ$ region around Tycho. The map has been obtained including all the contributions from the backgrounds (point sources and diffuse) except Tycho: a bright spot (TS = 33) is visible in the center of the map, which corresponds to the *Fermi*-LAT detection of Tycho. Another peak labeled BKG_Source in Figure 1, approximately one degree away from Tycho, is visible and has been added to the model.

The position of the source is obtained using a second maximum likelihood fitting package developed in the LAT Collaboration called *pointlike* (Kerr 2011), following Abdo et al. (2011) and selecting events above 1 GeV. The results of the localization are R.A. $= 00^{\rm h}25^{\rm m}37\overset{\rm s}{.}00$ and decl. $= +64^\circ06'56\overset{''}{.}0$ with a 95% error ellipse of $4\overset{'}{.}5 \times 3\overset{'}{.}8$ with the major axis inclined at 140° from the north toward the east. Systematic uncertainties are estimated to be about $0\overset{'}{.}3$. The 95% error ellipse is shown in Figure 2. The best-fit position is slightly offset toward the southeast of the remnant, but is compatible with the center.

We compared the best fit with a point-like source described above with the fit assuming the GeV emission follows the *XMM-Newton* map between 4.5 and 5.8 keV (mostly synchrotron). The point-like TS is only marginally better (by 3.3). We conclude that the X-ray synchrotron map is fully compatible with the *Fermi*-LAT data.

Concerning the spectral properties, the overall fit from 400 MeV to 100 GeV yields a TS of 33 for Tycho, which corresponds to a detection of about 5σ for point-like sources with 4 dof. The measured integral flux is $(3.5 \pm 1.1_{\rm stat} \pm 0.7_{\rm syst}) \times 10^{-9}$ cm^{-2} s^{-1} with a photon index of $2.3 \pm 0.2_{\rm stat} \pm 0.1_{\rm syst}$. The additional background source at R.A., decl. $= (00^{\rm h}15^{\rm m}45\overset{\rm s}{.}60, +63^\circ56'24\overset{''}{.}0)$ has a comparable overall flux of $(3.3 \pm 2.0_{\rm stat}) \times 10^{-9}$ cm^{-2} s^{-1} with a softer photon index of $2.4 \pm 0.2_{\rm stat} \pm 0.1_{\rm syst}$. Its significance is 5σ.

In order to obtain a spectral energy distribution (SED) the entire energy range has been divided into logarithmically evenly spaced energy bins from 400 MeV to 100 GeV. All the point sources in the RoI and the scale factors for the diffuse components in each bin have been then fitted using gtlike. The results of this band-by-band fitting procedure are shown in Figure 3 for Tycho. In this figure the data points are drawn with statistical uncertainties only; the systematics have been indicated with dashed boxes, calculated making the same fit with different IRFs (the Monte Carlo based P6V3 and the in-flight corrected P6V11) and different models of the Galactic and isotropic diffuse emission optimized for each IRF.

4. DISCUSSION

4.1. Association

A point-like GeV γ-ray source is found in the direction of Tycho's SNR based on more than 2.5 years of observation with *Fermi*-LAT. The positional coincidence between the *Fermi*-LAT γ-ray emission and Tycho's SNR suggests that the γ-ray emission is produced by shock-accelerated particles within the remnant. We have also considered the possibility of having a γ-ray

[7] http://fermi.gsfc.nasa.gov/ssc/
[8] http://fermi.gsfc.nasa.gov/ssc/data/access/lat/BackgroundModels.html
[9] The Test Statistic is defined as TS = 2(log(L_1)–log(L_0)) with L_0 the likelihood of the Null-hypothesis model (no point source present) as compared to the likelihood of a competitive model and L_1 as explained in Abdo et al. (2010a).

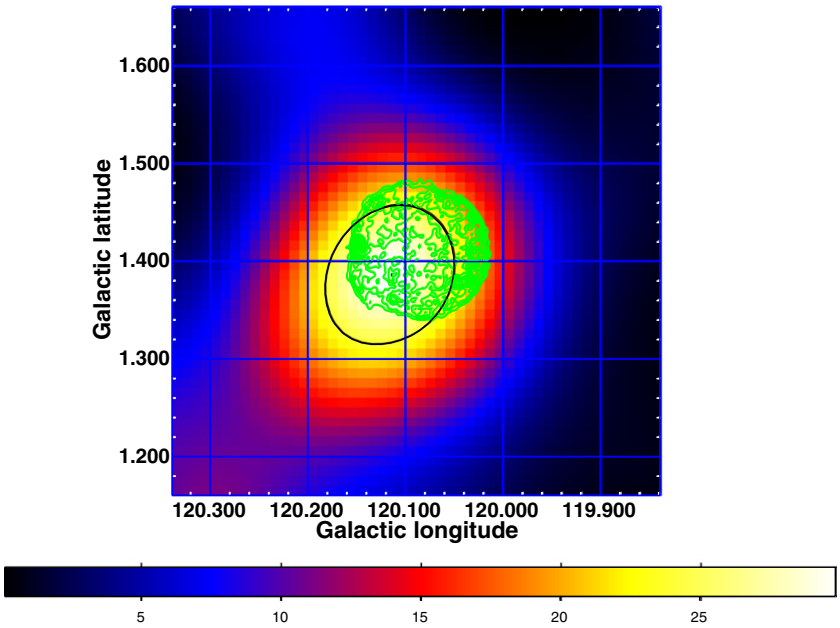

Figure 2. *Fermi*-LAT TS map zoomed in. The green contours are 4.5 keV–5.8 keV continuum band from *XMM-Newton* (Decourchelle et al. 2001) and the black line denotes the 95% confidence area for the *Fermi*-LAT position.
(A color version of this figure is available in the online journal.)

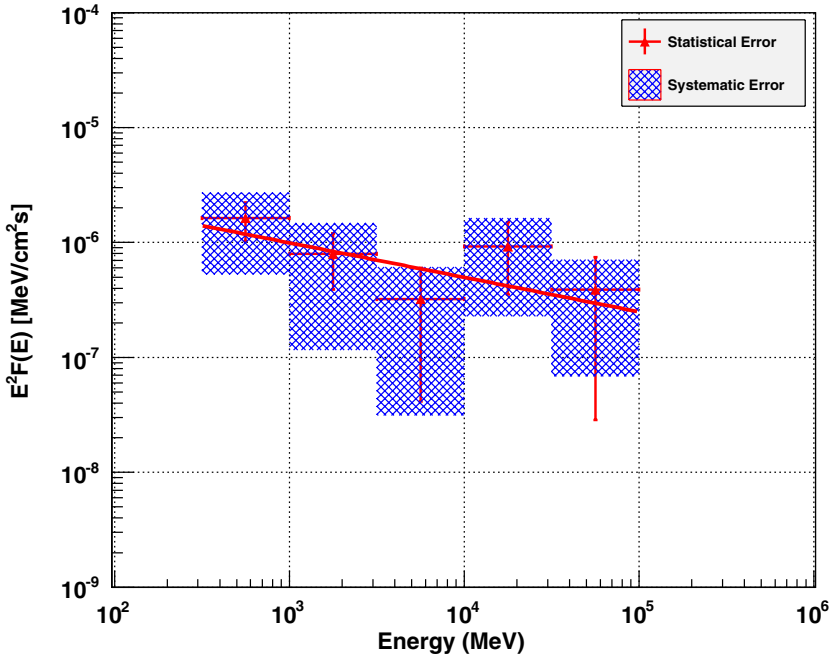

Figure 3. Spectrum obtained by evaluating the flux in separate energy bins. The shadowed regions indicate the uncertainties due to systematics in the effective area and in the accuracy of the modeling of the Galactic diffuse emission. The solid line reproduces the best fit for a power-law model.
(A color version of this figure is available in the online journal.)

emission from a pulsar which is the class of the most numerous Galactic objects. We have excluded this possibility considering that Tycho's SNR is known to be the result of a Type Ia explosion (Ruiz-Lapuente et al. 2004; Krause et al. 2008) and that the closest radio pulsar in the line of sight, PSR J0026+6320 (about 0.°8 from Tycho), has a dispersion measure distance of about 13.6 kpc with a spin-down power of approximately 2×10^{32} erg s^{-1}. Moreover, the γ-ray spectrum measured with the *Fermi*-LAT does not resemble the spectrum of a typical pulsar usually featuring an exponential cutoff (Abdo et al. 2010c). Also, the chance probability of finding an active galactic nucleus (AGN; the most populated class of LAT sources) within the 95% confidence contour has been investigated. The surface density of an AGN with an integral flux equivalent to that measured for Tycho or even greater is less than 8×10^{-3} deg^{-2} (Abdo et al. 2010b); therefore, the chance probability of finding one within $5'$ is less than 1.7×10^{-4}.

4.2. General Constraints

We consider the GeV γ-ray production from the bulk of the SNR (not the special eastern region). Cassam-Chenaï et al.

(2007) have analyzed the blast wave of Tycho in the framework of a model that accounts for the dynamical effect of diffusive shock acceleration and is broadly consistent with the location of the ejecta that requires the shock compression at the blast wave to be ∼6. That model assumes a self-similar evolution driven by ejecta distributed as r^{-7}, consistent with the expansion measurements of Reynoso et al. (1999) and Katsuda et al. (2010). Truelove & McKee (1999) have shown that the blast wave radius follows the self-similar solution up to twice the time when the reverse shock reaches the central plateau. So, that solution is valid for densities considered below up to a distance of 4 kpc or so.

As discussed in the Introduction, the main uncertainty is the distance to the source. Therefore, we need to extract the explicit dependence of the observational constraints on distance (expressed in kiloparsecs) $D_{\rm kpc}$. The explosion energy E_{51} (in units of 10^{51} erg) and ambient density $n_{\rm H}$ are not precisely known either.

In the self-similar model, the shock radius follows $R_{\rm sh}^7 \propto E_{51}^2/n_{\rm H}t^4$. Reproducing the angular radius of Tycho at the present time (4.′26 in the west) results in a generalization of Table 5 of Cassam-Chenaï et al. (2007) to any explosion energy:

$$n_{\rm H} = 388 D_{\rm kpc}^{-7} E_{51}^2 \ {\rm cm}^{-3}. \quad (1)$$

The absence of a clear detection of thermal X-ray emission from the shocked ambient gas led Cassam-Chenaï et al. (2007) to a constraint on density, namely, $n_{\rm H} < 0.3$ cm^{-3} at a distance of 2.8 kpc. That constraint was based on X-ray brightness and it does not depend very much on temperature, so it depends little on E_{51}. Since X-ray brightness is proportional to $\int n^2 dl$ along the line of sight, the main dependence is as $n_{\rm H}^2 D_{\rm kpc}$. Therefore, the constraint can be generalized to $n_{\rm H} < 0.3(2.8\ {\rm kpc}/D)^{0.5}$ cm^{-3}.

We also account for the fact that the total available energy at the blast wave $E_{51}^{\rm amb}$ is not the full explosion energy, as some of it is still locked up in the ejecta. The energy in the shocked gas is what was originally kinetic energy of the ejecta beyond the ejecta velocity at the reverse shock. In the self-similar phase, $E_{51}^{\rm amb}$ is 71% of it (the rest is shocked ejecta). Putting all this together,

$$E_{51}^{\rm amb} = 0.24 n_{\rm H}^{1/2} D_{\rm kpc}^{3/2} E_{51}. \quad (2)$$

Extrapolating that formula beyond the time at which the reverse shock enters the central plateau is reasonable. The transfer of energy to the shocked ambient gas continues, coming then from the shocked ejecta. $E_{51}^{\rm amb}/E_{51}$ would be 0.93 at the end of the validity of the self-similar phase defined above, so this approximation connects smoothly to the Sedov phase in which $E_{51}^{\rm amb} = E_{51}$.

For either bremsstrahlung or π^0 decay, both of which use the same target gas, the predicted γ-ray flux will be

$$F_\gamma \propto f_{\rm CR} E_{51}^{\rm amb} 3 n_{\rm H} D_{\rm kpc}^{-2} \propto 0.72 f_{\rm CR} E_{51} n_{\rm H}^{3/2} D_{\rm kpc}^{-1/2}, \quad (3)$$

where we have used Equation (2), and $f_{\rm CR}$ is the fraction of the available energy going into accelerated particles.

Equations (1) and (3) define, as a function of distance, a family of solutions in which n_0 decreases as $D_{\rm kpc}^{-3/2}$ and E_{51} increases as $D_{\rm kpc}^{11/4}$.

4.3. γ-Ray Emission

There are three radiation processes potentially responsible for the GeV γ-rays from (or in the direct vicinity of) Tycho's SNR: inverse Compton (IC) scattering on the cosmic microwave background (CMB) by relativistic electrons; non-thermal bremsstrahlung by relativistic electrons; and π^0-decay γ-rays resulting mainly from inelastic collisions between relativistic protons and ambient gas nuclei (Gaisser et al. 1998).

Two different cases are considered in the following: in the first case, called the "nearby" scenario, the total energy output of the supernova will be fixed to a standard value of 10^{51} erg, which results in a distance of 2.78 kpc assuming the maximally allowed value for the ambient density of 0.3 cm^{-3}. In the second case, we place the remnant at a distance of 3.5 kpc and calculate the supernova energy and its ambient density to be 2×10^{51} erg and 0.24 cm^{-3}, respectively. This constitutes the "far" scenario.

In both cases, the synchrotron flux is constrained by the radio and X-ray data. These data imply that a population of shock-accelerated electrons described by a power-law spectrum with a spectral index of 2.2–2.3 and a cutoff energy of 6–7 TeV is the origin of the observed synchrotron emission if we assume the downstream magnetic field to be $B_{\rm d} \sim 215\ \mu$G as inferred by X-ray measurements (Cassam-Chenaï et al. 2007). Since the magnetic field strength is the only parameter to determine the strength of the IC flux produced by the above-mentioned population of electrons on the CMB radiation and IR photon fields, the IC flux at ∼1 GeV is inevitably far below the observed value.

Could leptonic models account for the observed emission in Tycho's SNR? Given the spectral shape of the γ-ray emission, bremsstrahlung is the most likely way to fit the data in a leptonic model. The flux of bremsstrahlung γ-rays scales with the electron population and $n_{\rm H}$. Since the electron population cannot be increased too much, otherwise the IC contribution would quickly exceed that implied by the TeV data, the ambient density needs to be increased, and the downstream magnetic field has to be decreased to 65 μG. In the most favorable case of the "nearby" scenario the required gas density would be $n_{\rm H} = 9.7$ cm^{-3} (using an effective density twice larger behind the shock, as prescribed by a Sedov model). This value exceeds the gas density allowed by X-ray measurements by a factor of 30 (Cassam-Chenaï et al. 2007). Moreover, given the extremely high gas density, the energy in the accelerated hadrons must not exceed 1.5×10^{48} erg which would correspond to an extremely high value of $K_{\rm ep} = 0.1$. In this case the SNR has to be in the Sedov phase and thus the supernova energy would be 4.4×10^{51} erg, which is exceptionally high for a Type Ia supernova.

The left panel of Figure 4 shows a leptonic scenario in which the γ-ray emission is generated by IC scattering of CMB photons assuming a magnetic field of 30 μG. The ambient density is assumed to be the same as in the hadronic scenario (already the maximum allowed value) and yields a bremsstrahlung flux that underestimates the low-energy part of the measured LAT spectrum. While a leptonic model can reproduce the γ-ray flux, it does not fit the spectral shape well. Even considering optical and IR photon fields of reasonable intensities, the GeV–TeV spectrum cannot be accounted for by leptonic emission. For all these reasons the bremsstrahlung and IC channel is very unlikely to account for the *Fermi*-LAT measurement.

On the other hand, the expected γ-ray spectrum of hadronic origin can be calculated on the assumption that efficient proton acceleration is taking place at the forward shock in Tycho's SNR, whereby the protons acquire the same power-law spectrum with the same spectral index as the aforementioned electron

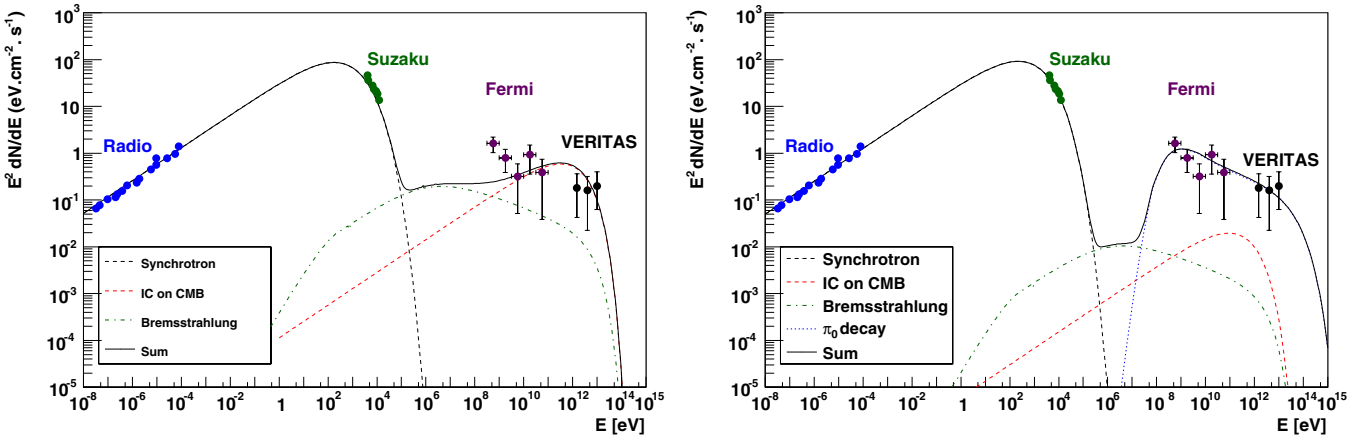

Figure 4. Broadband SED model of Tycho's SNR for the far scenario in leptonic model (left) and hadronic interpretation (right).
(A color version of this figure is available in the online journal.)

Table 1
Parameters Used in the Spectral Energy Modeling Shown in Figure 4

Case	$D_{\rm kpc}$ (kpc)	$n_{\rm H}$ ($\rm cm^{-3}$)	$E_{\rm SN}$ (10^{51} erg)	$E_{p,\rm tot}$ (10^{50} erg)	$E_{e,\rm tot}$ (erg)
Far leptonic	3.50	0.24	2.0	-	1.5×10^{48}
Far hadronic	3.50	0.24	2.0	1.50	6.7×10^{46}
Nearby hadronic	2.78	0.30	1.0	0.61	4.3×10^{46}

Note. Spectral indices have been fixed to 2.3 for both electrons and protons.

spectrum. Only the cutoff energy is much higher as protons do not suffer from synchrotron losses as much as electrons do. Since the VERITAS spectral measurements (Acciari et al. 2011) do not indicate any cutoff, we estimate the maximum proton energy by equating the acceleration time (assuming Bohm diffusion) with the age of Tycho. For $B_{\rm d} = 215\ \mu$G, this results in an energy break for protons of $E_{p,\rm max} = 44\ D_{\rm kpc^2}$ TeV (Parizot et al. 2006).

The intensity of this emission depends on the total energy in the accelerated protons (and other ions) as well as on the density of the ambient medium $n_{\rm H}$. Even though the density is expected to be around 6 $n_{\rm H}$ just behind the shock front, the average density seen by the shock-accelerated protons over the full emission zone between the blast wave and the ejecta is only around 3 $n_{\rm H}$ in the self-similar model.

Furthermore, the γ-ray emission has been computed assuming that shock acceleration is not very efficient and only 10% of the available energy eventually gets transferred into the protons/cosmic rays ($E_{51}^{\rm amb} = 0.77 E_{51}$ or $0.61 E_{51}$ in the "far" or "nearby" case, respectively, from Equation (2))

The relevant parameters for the two different cases used here are summarized in Table 1. As shown in the right panel of Figure 4, this conventional hadronic model can explain very well the whole γ-ray emission from the GeV to the TeV part of the spectrum in a way consistent with all the constraints.

5. CONCLUSIONS

A 5σ detection of GeV γ-ray emission from Tycho's SNR is reported. The flux above 400 MeV is $(3.5 \pm 1.1_{\rm stat} \pm 0.7_{\rm syst}) \times 10^{-9}$ $\rm cm^{-2}$ $\rm s^{-1}$ and the photon index $2.3 \pm 0.2_{\rm stat} \pm 0.1_{\rm syst}$. The measured *Fermi* spectrum as well as the available radio, X-ray, and TeV data can be explained by an accelerated proton population which produces γ-ray photons via π^0 production and decay. IC emission and bremsstrahlung can account for only a fraction of the observed γ-ray flux.

The *Fermi*-LAT Collaboration acknowledges support from a number of agencies and institutes for both development and the operation of the LAT as well as scientific data analysis. These include NASA and DOE in the United States, CEA/Irfu and IN2P3/CNRS in France, ASI and INFN in Italy, MEXT, KEK, and JAXA in Japan, and the K. A. Wallenberg Foundation, the Swedish Research Council, and the National Space Board in Sweden. Additional support from INAF in Italy and CNES in France for science analysis during the operations phase is also gratefully acknowledged.

REFERENCES

Abdo, A. A., Ackermann, M., Ajello, M., et al. 2009, Phys. Rev. D, 80, 122004
Abdo, A. A., Ackermann, M., Ajello, M., et al. 2010a, ApJS, 188, 405
Abdo, A. A., Ackermann, M., Ajello, M., et al. 2010b, ApJ, 720, 435
Abdo, A. A., Ackermann, M., Ajello, M., et al. 2010c, ApJS, 187, 460
Abdo, A. A., et al. 2011, ApJS, submitted (arXiv:1108.1435)
Acciari, V. A., Aliu, E., Arlen, T., et al. 2011, ApJ, 730, L20
Atwood, W. B., Abdo, A. A., Ackermann, M., et al. 2009, ApJ, 697, 1071
Cassam-Chenaï, G., Hughes, J. P., Ballet, J., & Decourchelle, A. 2007, ApJ, 665, 315
Chevalier, R. A. 1982, ApJ, 258, 790
Decourchelle, A., Sauvageot, J. L., Audard, M., et al. 2001, A&A, 365, L218
Fink, H. H., Asaoka, I., Brinkmann, W., Kawai, N., & Koyama, K. 1994, A&A, 283, 635
Gaisser, T. K., Protheroe, R. J., & Stanev, T. 1998, ApJ, 492, 219
Hayato, A., Yamaguchi, H., Tamagawa, T., et al. 2010, ApJ, 725, 894
Katsuda, S., Petre, R., Hughes, J. P., et al. 2010, ApJ, 709, 1387
Kerr, M. 2011, PhD thesis, Univ. Washington
Kothes, R., Fedotov, K., Foster, T. J., & Uyanıker, B. 2006, A&A, 457, 1081
Krause, O., Tanaka, M., Usuda, T., et al. 2008, Nature, 456, 617
Lee, J.-J., Raymond, J. C., Park, S., et al. 2010, ApJ, 715, L146
Parizot, E., Marcowith, A., Ballet, J., & Gallant, Y. A. 2006, A&A, 453, 387
Petre, R., Allen, G. E., & Hwang, U. 1999, Astron. Nachr., 320, 199
Rest, A., Welch, D. L., Suntzeff, N. B., et al. 2008, ApJ, 681, L81
Reynoso, E. M., Velázquez, P. F., Dubner, G. M., & Goss, W. M. 1999, AJ, 117, 1827
Ruiz-Lapuente, P., Comeron, F., Méndez, J., et al. 2004, Nature, 431, 1069
Tian, W. W., & Leahy, D. A. 2011, ApJ, 729, L15
Truelove, J. K., & McKee, C. F. 1999, ApJS, 120, 299
Warren, J. S., Hughes, J. P., Badenes, C., et al. 2005, ApJ, 634, 376